

# Parametric Study of 3D Micro-Fin Tubes on Heat Transfer and Friction Factor

Shima Soleimani, Steven Eckels

**Abstract**—One area of special importance for the surface-level study of heat exchangers is tubes with internal micro-fins (< 0.5 mm tall). Micro-finned surfaces are a kind of extended solid surface in which energy is exchanged with water that acts as the source or sink of energy. Significant performance gains are possible for either shell, tube, or double pipe heat exchangers if the best surfaces are identified. The parametric studies of micro-finned tubes that have appeared in the literature left some key parameters unexplored. Specifically, they ignored three-dimensional (3D) micro-fin configurations, conduction heat transfer in the fins, and conduction in the solid surface below the micro-fins. Thus, this study aimed at implementing a parametric study of 3D micro-finned tubes that considered micro-fine height and discontinuity features. A 3D conductive and convective heat-transfer simulation through coupled solid and periodic fluid domains is applied in a commercial package, ANSYS Fluent 19.1. The simulation is steady-state with turbulent water flow cooling the inner wall of a tube with micro-fins. The simulation utilizes a constant and uniform temperature on the tube outer wall. Performance is mapped for 18 different simulation cases, including a smooth tube using a realizable  $k-\epsilon$  turbulence model at a Reynolds number of 48,928. Results compared the performance of 3D tubes with results for the similar two-dimensional (2D) one. Results showed that the micro-fine height has a greater impact on performance factors than discontinuity features in 3D micro-fin tubes. A transformed 3D micro-fin tube can enhance heat transfer, and pressure drops up to 21% and 56% compared to a 2D one, respectfully.

**Keywords**—Three-dimensional micro-fin tube, heat transfer, friction factor, heat exchanger.

## I. INTRODUCTION

**M**ICRO-FIN surfaces are an important class of internally enhanced surfaces in commercial applications such as air conditioners, refrigeration evaporators, and condensers. A typical performance goal for internal flow over micro-finned surfaces is to increase heat-transfer with a minimum pressure drop penalty. Current commercial practice of design for water-based systems is to use trapezoidal micro-fins on tube heat-exchange surfaces. Fig. 1 shows an internally micro-finned tube.

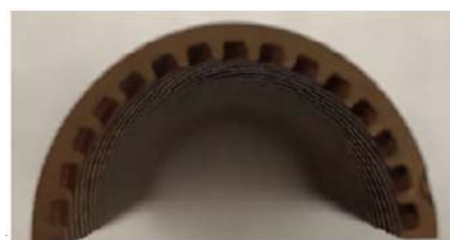
Few numerical studies are devoted to researching the performance of internal micro-fins in tube heat exchangers and they are only based on 2D helical micro-fins [2]-[8], while experimental studies have proved the performance of 3D micro-finned tubes surpasses the 2D ones [9]-[11]. Takahashi et al. [10] showed that a specified 3D micro-finned tube (A-8) with water flow not only enhanced heat transfer rate with

relatively low pressure drop, but also reduced the surface area of a shell and tube evaporator by 27% which was not achievable using 2D micro-fin tubes. Webb et al. [11] studied the performance of three different types of 3D cone micro-fin tubes with water flow and compared the results with the best available commercially reported 2D micro-fin tube (Turbo BIII). They showed that two tubes of three cone micro-fin tubes had 14% to 20% greater heat transfer enhancement and nearly 5% greater performance factor than the Turbo BIII tube.

A surface-level design study of tube heat exchanger using passive methods requires both conduction and convection heat transfer analysis. However, most finned tube studies ignored the conduction analysis of the fin and solid domain that fins are attached to. The only exception is [7] which was limited to 2D micro-fin tubes. Therefore, this study tries to cover the research gap by applying a fast and accurate computational fluid dynamic (CFD) model to simulate turbulent water flow with heated solid domain to study the effective parameters of a 3D micro-fin tube on heat transfer and friction factor.



(a)



(b)

Fig. 1 (a) Longitudinal and (b) lateral cross-section of an internally micro-fin tube [1]

## II. PROBLEM DEFINITION

### A. Design Parameters

This study aims to gain better performance by turning 2D micro-finned tubes to a 3D ones by changing micro-fin height

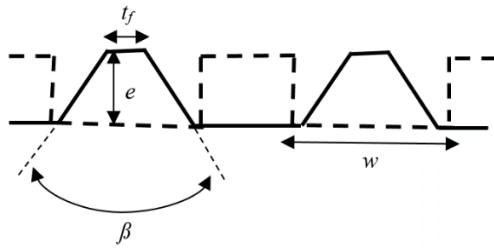
Shima Soleimani is with the Kansas State University, USA (e-mail: shimasoleimani@ksu.edu).

and discontinuity features. The main design parameters of an internally 3D micro-finned tube are micro-fin cross-section profile, helix angle ( $\alpha$ ), height ( $e$ ), number of starts ( $n_f$ ), and discontinuity features. Numerical results by [7] and [8] highlighted negligible effect of micro-fin cross-sectional profiles on heat transfer or pressure drop. Therefore, this study justified a constant micro-fin trapezoidal profile ( $\beta = 41^\circ$ ), micro-fin width ( $t_f = 0.12$  mm), inner tube diameter ( $D_i = 15.54$  mm) and outer tube diameter ( $D_o = 19$  mm) reported by [11]. This study considers the micro-fin discontinuity features by defining cutter number of starts ( $n_c$ ) and cutter width ( $w$ ). The number of discontinuities along a micro-fin pitch is calculated by  $\delta = n_f/n_c$ . In this study, a 2D micro-fin configuration is transformed in to a 3D micro-fin configuration when  $n_c$  or  $w$  take non-zero values. Fig 2 illustrates design parameters for a 3D micro-fin tube.

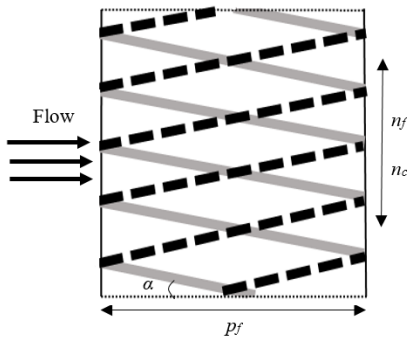
The parameters of  $\alpha$  and  $n_f$  are related to axial micro-fin pitch ( $p_f$ ) as follows:

$$p_f = \frac{\pi D_i}{n_f \tan(\alpha)} \quad (1)$$

An axial cutter pitch (pc) is equal to  $(1/\eta) \times p_f$ .



(a)



(b)

Fig. 2 A schematic of (a) micro-fin and cutter profiles and (b) an unrolled tube with micro-fins and cutters (solid line for micro-fin and dash lines for cutter representation)

This study considers design parameters of  $e = 0.1, 0.3, 0.5$  mm,  $\alpha = 25^\circ$ ,  $n_f = 30$ ,  $n_c = 0, 15, 30$ , and  $w = 0, 0.5, 1, 1.5$  mm. The reason to choose helix angle of constant  $25^\circ$  and number of starts of 30 is for comparison with the experimental results reported by [3] for the best parameters of a 2D micro-fin tube.

Table I shows the combination of designed parameters for creating the 2D and 3D micro-finned tubes due to geometrical constraints.

TABLE I  
DESIGNED PARAMETERS FOR 2D AND 3D MICRO-FINDED TUBES

$e$ (mm)	$\alpha$ ( $^\circ$ )	$n_f$	$n_c$	$w$ (mm)
0.1	25	30	0	0.0
0.1	25	30	15	0.5
0.1	25	30	15	1.0
0.1	25	30	15	1.5
0.1	25	30	30	0.5
0.1	25	30	30	1.0
0.3	25	30	0	0.0
0.3	25	30	15	0.5
0.3	25	30	15	1.0
0.3	25	30	15	1.5
0.3	25	30	30	0.5
0.3	25	30	30	1.0
0.5	25	30	0	0.0
0.5	25	30	15	0.5
0.5	25	30	15	1.0
0.5	25	30	15	1.5
0.5	25	30	30	0.5
0.5	25	30	30	1.0

### B. Evaluation Criteria

This study applies the evaluation criteria of performance factor which is defined as the ratio  $j$ -factor increase to friction factor increase compared to a smooth surface. The factor is calculated as:

$$\eta = \frac{j/j_s}{f/f_s} = \frac{(St Pr^{2/3})/(St Pr^{2/3})_s}{f/f_s} \quad (2)$$

in which,  $St$  is Stanton number,  $Pr$  is Prandtl number,  $f$  is fanning friction factor, and the subscription of  $s$  refers to smooth surface.

### III. SIMULATION SETUP

A coupled numerical simulation of turbulent flow with periodic boundaries and solid domains was set up and validated in ANSYS Fluent. Numerical simulation of conductive heat transfer through solid domain while coupling with convective heat transfer requires solution of continuity equation, energy conservation equation, and Navier-Stokes equations of motion. The equations for incompressible flow and constant fluid properties are computed as:

$$\nabla \cdot \bar{V} = 0 \quad (3)$$

$$\rho \frac{D\bar{V}}{Dt} = \rho \bar{g} - \nabla p + \mu \nabla^2 \bar{V} \quad (4)$$

$$\rho c_p \frac{DT}{Dt} = \rho \dot{q}_s + k \nabla^2 T + \mu \left[ \nabla \bar{V} + (\nabla \bar{V})^T \right] : \nabla \bar{V} \quad (5)$$

where,  $\vec{V}$  is velocity vector;  $\rho$  is density;  $t$  is time;  $\vec{g}$  is gravitational acceleration;  $p$  is pressure;  $\mu$  is dynamic viscosity;  $c_p$  is specific heat at constant pressure;  $\dot{q}_g$  is rate of heat generation per unit volume;  $k$  is thermal conductivity; and  $T$  is temperature.

This study applies the Reynolds-averaged Navier–Stokes equations (RANS) using realizable  $k$ - $\epsilon$  turbulence model and an enhanced wall function method. Translational periodic boundary conditions were applied to obtain solutions in the fully developed region of the flow. In this condition, a tiny domain is solved repeated times as flow over the region evolves to the fully developed solution. A CFD flow solver using pressure-based method was chosen to achieve pressure field solution. This study applies a pressure-velocity coupling equation to discretize Navier-Stokes equations with a coupled scheme combination.

#### A. Properties and Boundary Conditions

This study applies the following assumption/constant parameters to simulate the flow through the heated domain.

- Flow is assumed 3D, turbulent, incompressible, fully developed, and steady state;
- The inlet flow temperature is at 293.15 K;
- The inlet mass flow rate is set at 0.598 kg/s that based on the defined tube diameter leads to a Reynolds number of 48,928;
- The thermodynamics variables are temperature independent and assumed constant:  $\rho = 998.2 \text{ kg/m}^3$ ,  $\mu = 0.001003 \text{ kg/(m.s)}$ ,  $k = 0.6 \text{ W/(m.K)}$ , and  $c_p = 4182 \text{ J/(kg.K)}$ ; and,
- The tube's outer wall temperature was at 313.15 K.

#### B. Geometry

In order to reach a 3D micro-finned tube, first trapezoidal micro-fin profiles are extruded with right-handed helix along tube surface to make a 2D micro-fin configuration, then rectangular cutter profiles are extruded with left-handed helix along the tube inner surface and axially cut the micro-fins on their extension. Fig. 3 represents the internally 2D and 3D micro-finned tubes.

#### C. Meshing

For discrete representation of the geometry, an unstructured tetrahedral grid system is used to generate the mesh. In the fluid section, the height of first grid points is set at  $0.003D_i$  from the wall to satisfy the dimensionless distance from the wall ( $y^+$ ) less than 5. Fig. 4 shows an example of grid system for a micro-finned tube case.

To eliminate the effects of mesh refinement on the results, mesh independency analysis was performed to find the optimum grid size for the present study for a smooth and micro-fin tubes. Fig. 5 shows the number of mesh elements for model convergence due to  $j$ -factor and friction factor for a micro-fin tube. It has been discovered that there is no remarkable change beyond  $25 \times 10^5$  elements for both  $j$ -factor and friction factor. Hence, this study applied this grid size to carry out the simulations for different cases of micro-finned

tubes.

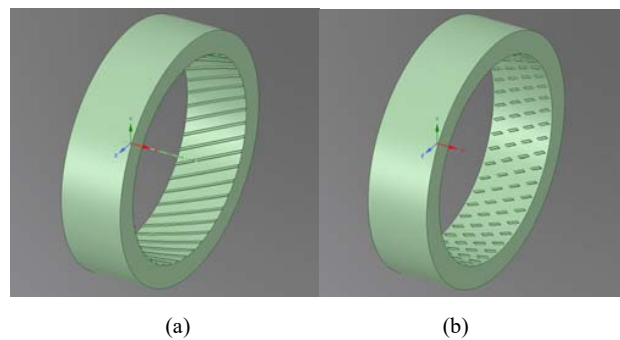


Fig. 3 Geometry presentation of (a) 2D and (b) 3D micro-finned tubes

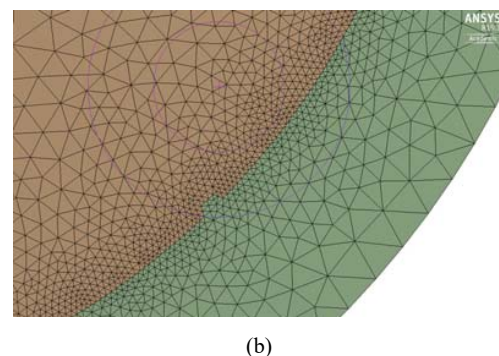
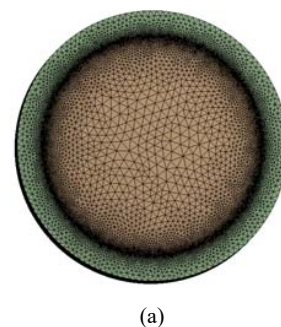


Fig. 4 Grid system of (a) whole domain and (b) zoom-in view at the solid and fluid interface for a micro-finned tube with  $e = 0.1 \text{ mm}$

## IV. RESULTS

#### A. Tube Validation

The numerical results were validated with experimental results reported by [11] for Tube 1 (a smooth tube) and Tube 7 with  $e = 0.532 \text{ mm}$ ,  $\alpha = 25$ ,  $n_f = 25$  at  $Re = 48,928$ . Table II shows the numerical and experimental results of  $j$ -factor and friction factor. The relative error of numerical and experimental results for both the smooth and micro-fin tubes confirmed that the model accuracy is good enough for the purpose of this study.

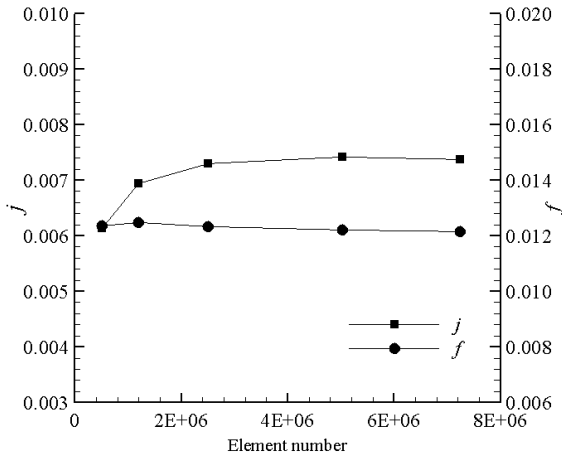


Fig. 5  $j$ -factor and friction factor results for different grid size of a micro-fined tube

TABLE II  
COMPARISON OF NUMERICAL AND EXPERIMENTAL RESULTS FOR TUBE 1 AND TUBE 7

Tube number	$f_{sim}$	$f_{exp}$	$f_{error} (%)$	$j_{sim}$	$j_{exp}$	$j_{error} (%)$
1	0.0052	0.0057	7.5	0.0036	0.0032	-13.9
7	0.0080	0.0090	8.2	0.0056	0.0059	4.9

**B. Tube Performance**

Performance is mapped for the different 18 micro-fin tube cases. Fig. 6 shows the effects of micro-fin height and discontinuity features on performance factor for different micro-fin height. It is observed that the most effective parameter is micro-fin height. Both 2D and 3D micro-fins with lowest height ( $e = 0.1$  mm) have the greatest performance factors. It is discovered that the effects of discontinuity length are increasing with micro-fin height. The increase of discontinuity length obviously decays performance factor at  $e = 0.3$  and  $0.5$  mm. Generally, micro-fins with cutter number of starts of 15 have better performance factor than cutter number of starts of 30. The greatest performance factor ( $\eta = 1.11$ ) belongs to a 3D micro-fin tube with  $e = 0.1$  mm,  $n_c = 15$ , and  $w = 1$  mm. And, the lowest performance factor ( $\eta = 0.703$ ) is for a 3D micro-fin with  $e = 0.5$  mm,  $n_c = 30$ , and  $w = 1$  mm. The best 2D micro-fin tube has a performance factor of 1.10 with  $e = 0.1$  mm. Results showed that making 3D micro-fin tube out of a 2D micro-fined tube enhanced the performance factor only by 0.9% for the defined design parameters of this study.

Fig. 7 shows the relationship between four design parameters and enhancement on  $j$ -factor and friction factor. It appears that there is a strong relationship between micro-fin height and enhancement of  $j$ -factor and friction factor (Fig. 7 (a)). Besides, for the defined micro-fin helix angle and number of starts in this study,  $j$ -factor enhancement was always greater and lower than friction factor enhancement when height was 0.1 and 0.5 mm, respectively. According to Fig. 7 (b), 3D micro-fin tubes ( $n_c = 15$  and 30) had greater  $j$ -factor and friction factor increase compared to the 2D micro-fin tubes ( $n_c$

= 0). And, increasing cutter number of starts from 15 to 30 increased overall  $j$ -factor and friction factor enhancement. The highest  $j$ -factor enhancement (1.92) belongs to discontinuity length of 0.5 mm and the highest (2.53) and shortest (1.15) friction factor enhancement happened at  $w = 1$  mm and  $w = 0$  (refers to a 2D micro-fined tube), respectively (Fig. 7 (c)). Statistical result of the coefficient of determination ( $R^2 = 0.77$ ) showed that surface area increase of tubes had a roughly linear response with  $j$ -factor enhancement. But there is no rational linear relationship between friction factor enhancement and surface area increase since  $R^2$  was 0.55 (Fig. 7 (d)).

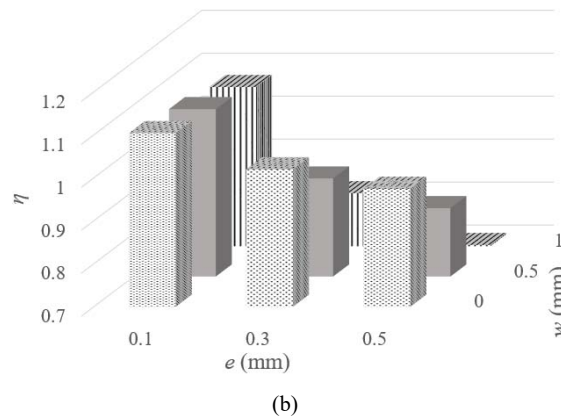
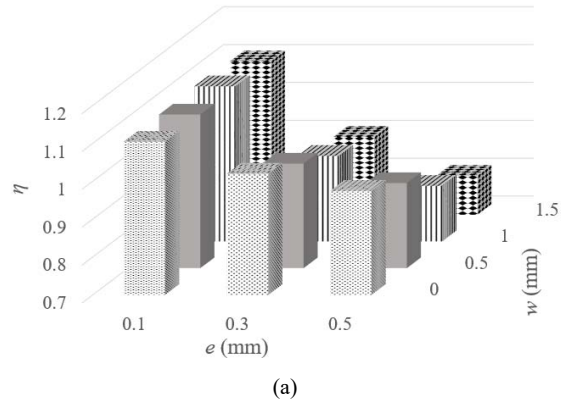


Fig. 6 Effect of micro-fin height and length of discontinuity on performance factor for (a) 15 and (b) 30 cutter number of starts

**V. CONCLUSION**

This paper provides numerical data for three 2D micro-fin tubes and 15 transformed 3D micro-fin tubes considering different micro-fin height and discontinuity features. Numerical data show a reasonable agreement with experimental data at a Reynolds number of 48,928. Micro-fin tube performance compares in terms of  $j$ -factor enhancement, friction factor enhancement, and performance factor. This study gained less than 1% enhancement of performance factor from a transformed 3D micro-fin tube in comparison to a 2D one.

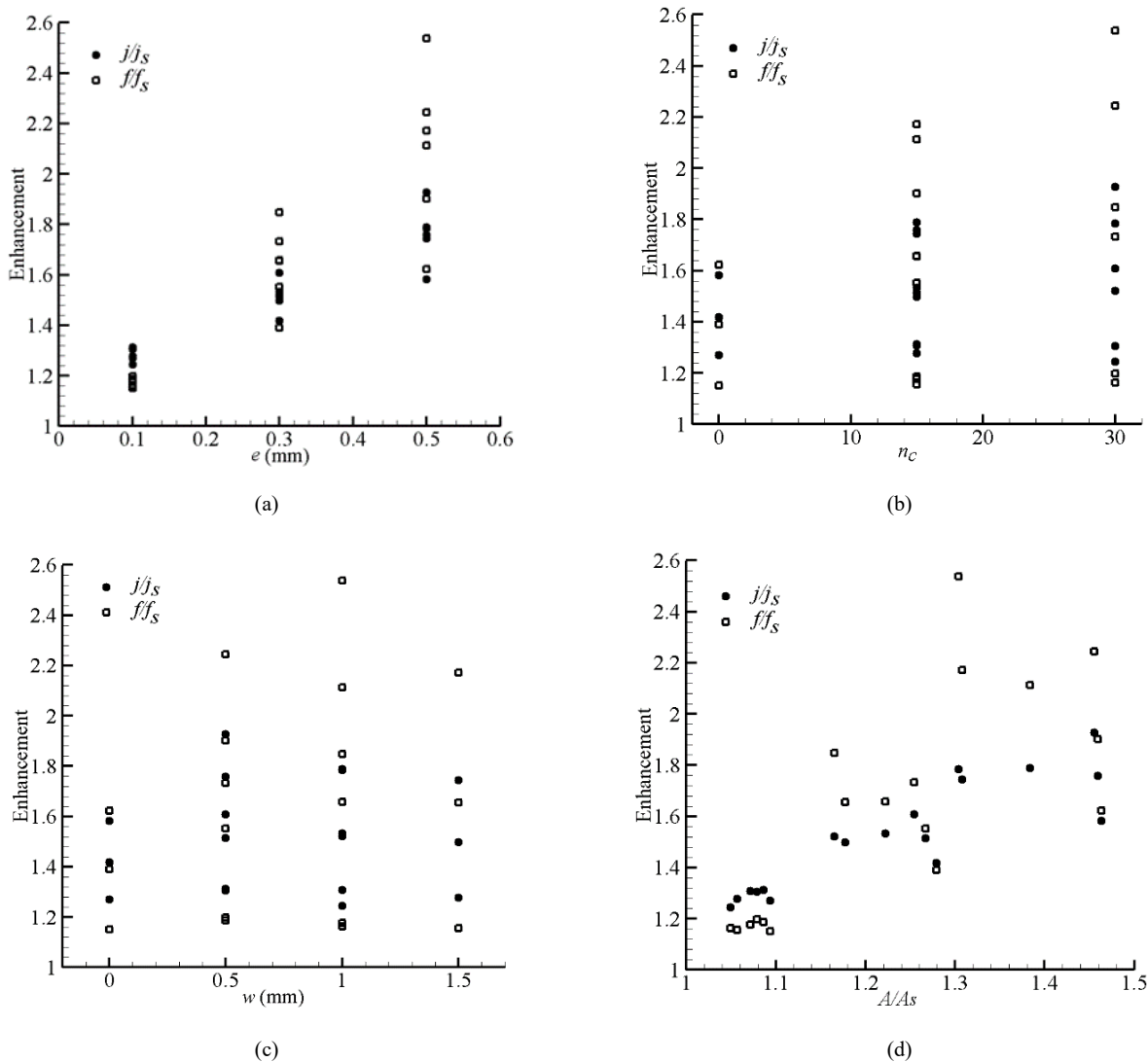


Fig. 7 Effect of (a) micro-fin height, (b) cutter number of stars, (c) micro-fin discontinuity length, and (d) surface area increase on enhancement of  $j$ -factor and friction factor

#### ACKNOWLEDGMENT

Support and internal funding from the Institute for Environmental Research (IER) is acknowledged.

#### REFERENCES

- [1] Li, P., 2019. Validation of large eddy simulations for modeling micro-structured enhanced heat transfer surfaces. Ph.D. dissertation, Department of Mechanical and Nuclear Engineering, Kansas State University, USA.
- [2] Mann, G.W. and Eckels, S., 2019. Multi-objective heat transfer optimization of 2D helical micro-fins using NSGA-II. *International Journal of Heat and Mass Transfer*, 132, pp.1250-1261.
- [3] Dastmalchi, M., Sheikhzadeh, G.A. and Arefmanesh, A., 2017. Optimization of micro-finned tubes in double pipe heat exchangers using particle swarm algorithm. *Applied Thermal Engineering*, 119, pp.1-9.
- [4] Bhatia, R.S. and Webb, R.L., 2001b. Numerical study of turbulent flow and heat transfer in micro-fin tubes—part 2, parametric study. *Journal of Enhanced Heat Transfer*, 8(5).
- [5] Campet, R., Roy, P.T., Cuenot, B., Riber, É. and Jouhaud, J.C., 2020. Design optimization of a heat exchanger using Gaussian process. *International Journal of Heat and Mass Transfer*, 150, p.119264.
- [6] Webb, R.L., 2009. Single-phase heat transfer, friction, and fouling characteristics of three-dimensional cone roughness in tube flow. *International Journal of Heat and Mass Transfer*, 52(11-12), pp.2624-2631.
- [7] Soleimani, S., Campbel, M. and Eckels, S., 2020. Performance analysis of different transverse and axial micro-fins in a turbulent-flow channel. *International Journal of Thermal Sciences*, 149, p.106185.
- [8] Soleimani, S. and Eckels, S.J., 2019. Effect of Micro-Fin Geometry on Liquid Heat Transfer Rate and Pressure Drop. In *ASTFE Digital Library*. Begel House Inc.
- [9] Brognaux, L.J., Webb, R.L., Chamra, L.M. and Chung, B.Y., 1997. Single-phase heat transfer in micro-fin tubes. *International Journal of Heat and Mass Transfer*, 40(18), pp.4345-4357.
- [10] Takahashi, K., Nakayama, W. and Kuwahara, H., 1988. Enhancement of forced convective heat transfer in tubes having three-dimensional spiral ribs. *Heat transfer. Japanese research*, 17(4), pp.12-28.
- [11] Webb, R.L., Narayanamurthy, R. and Thors, P., 2000. Heat transfer and friction characteristics of internal helical-rib roughness. *J. Heat Transfer*, 122(1), pp.1.